Available online at www.sciencedirect.com
ScienceDirect
International Journal of Heat and Mass Transfer 50 (2007) 4908–4911
International Journal of HEAT and MASS TRANSFER
www.elsevier.com/locate/ijhmt

Technical Note

Wall temperature measurements with turbulent flow in heated vertical circular/non-circular channels of supercritical pressure carbon-dioxide

Jong Kyu Kim, Hong Kyu Jeon, Joon Sik Lee *

School of Mechanical and Aerospace Engineering, Seoul National University, Seoul 151-742, Republic of Korea

Received 12 April 2006; received in revised form 10 January 2007
Available online 21 August 2007

Abstract

Experimental data are presented which illustrate heat transfer characteristics of the turbulent supercritical flow in vertical circular/non-circular channels. The working fluid was carbon-dioxide operating at a constant pressure of 8 MPa. Experiments were conducted at various conditions with inlet bulk fluid temperatures ranging from 15 to 32 °C, imposed heat fluxes from 3 to 180 kW/m^2, and mass fluxes from 209 to 1230 kg/m^2 s. The corresponding Reynolds numbers were within the range of 3×10^4 to 1.4×10^5. Wall temperatures are presented for the three channels with different cross-sectional shapes. These were measured by thermocouples installed on the outer surface of the heating section, and are compared with each other at the same heat flux and mass flux conditions.

Keywords: Turbulent flow; Supercritical pressure; Circular/non-circular channels; Carbon-dioxide; Heat transfer deterioration

1. Introduction

Supercritical pressure fluids have been practically utilized since 1950s in conventional fossil-fuel power plant. The thermal efficiency can be increased from 35% to about 45–50% in such plant. Additional benefits include simplified design of power plant compactness and cost reduction. For these reasons, recently, the usage of supercritical water is extended to the ultra-supercritical steam generators and applied to the supercritical water-cooled nuclear reactor and refrigerating systems.

At supercritical pressure, significant changes in thermophysical properties take place near the pseudocritical temperature. The working fluid undergoes a transition from liquid-like to gas-like behavior when the fluid temperature rises up and passes through the pseudocritical temperature. In addition, for vertically upward flow, the buoyancy force plays an important role in the development of turbulent wall-shear stress because of abrupt density variation near the wall, especially when the mass flux is low and the heat flux is high. Thus, the combined effects of property variation and buoyancy bring about significant impact on the heat transfer, which make it difficult to predict the heat transfer at supercritical conditions.

Until now, heat transfer experiments in non-circular channels have been conducted mainly with gas. Campbell and Perkins [1] and Battista and Perkins [2] tested the effects of variable thermophysical properties on local heat transfer coefficient for fully developed turbulent air flow in vertical non-circular channels. Campbell and Perkins [1] found that the local heat transfer coefficient in an equilateral duct is lower than that in a circular duct. In the investigation of heat transfer in a square duct, Battista and Perkins [2] observed that the local heat transfer coefficient was about the same as that in the equilateral triangular duct.

The objective of the present study is to examine the distinctive characteristics of supercritical heat transfer in non-circular channels with triangular and square cross-sections.

* Corresponding author. Tel.: +82 2 880 7117; fax: +82 2 883 0179.
E-mail address: jslee123@snu.ac.kr (J.S. Lee).

0017-9310/$ - see front matter © 2007 Elsevier Ltd. All rights reserved.
doi:10.1016/j.ijheatmasstransfer.2007.06.026

Nomenclature

D_{hy}	inner hydraulic-equivalent diameter of channel [m]
g	gravitational acceleration [m/s^2]
Gr	Grashof number, $g\beta_b qD^4/k_b v_b^2$
k	thermal conductivity [W/m K]
q	heat flux [W/m^2]
Re	Reynolds number, $\rho_b u_b D/\mu_b$
u	streamwise velocity [m/s]
x	streamwise coordinate

Greek symbols

β	volumetric expansion coefficient [K^{-1}]
μ	dynamic viscosity [kg/m s]
ρ	density [kg/m^3]
ν	kinematic viscosity [m^2/s]

Subscript

b	bulk condition

Wall temperature distributions for non-circular channels are presented along with those of circular channels.

2. Experiments

The schematic of the test facility is depicted in Fig. 1. It is composed of a main loop for carbon-dioxide flow and a secondary loop for cooling water. The working fluid is carbon-dioxide with 99.5% purity, which is pressurized to 8 MPa by using an air-driven booster pump and an accumulator. The working fluid is pumped round the main loop by a magnetic gear pump. The mass flow rate is controlled by changing the pump rpm and is measured by a Coriolis type flowmeter. The carbon-dioxide is delivered to the electric preheater and/or to the bypass line when it is necessary to adjust the flow rate or to stabilize the system. The electric preheater allows the fluid temperature to rise up automatically to a desired temperature at the inlet to the test section as listed in Table 1. After being heated above the pseudocritical temperature in the test section, the fluid cools down to a temperature lower than the inlet temperature when it passes through two shell-and-tube type coolers. The chiller is used for supplying the water to the two coolers at an appropriate flow rate and temperature.

The test channels were made of Inconel 625, and channel wall thickness was 1 mm for each of them. The hydraulic diameters of the circular, triangular, and square channels are 7.8 mm, 9.8 mm, and 7.9 mm, respectively. The test channels were mounted vertically to generate aiding mixed convection flows. To provide a uniform heat flux at the heating region of the test section, a DC heating method was adopted. The outer wall temperature variations along the test channels were measured by chromel–alumel sheath type thermocouples, which were electrically insulated. Forty-five thermocouples were silver-soldered to each wall of the circular and non-circular channels every 30 mm from the starting point of the heating region. The outer walls of the test channels were thermally well insulated by ceramic-wool which is suitable for the high temperature insulation, and wrapped by the ceramic-tape. To

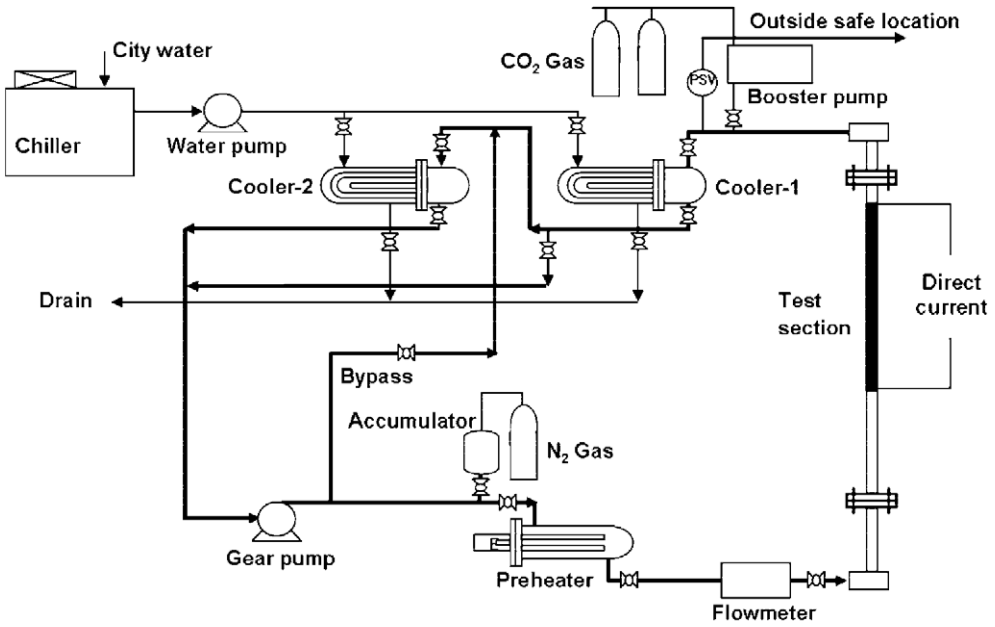

Fig. 1. Schematic of the test facility.

Table 1
Experimental conditions

Pressure [MPa]	8
Inlet fluid temperature [°C]	15, 25, 32
Heat flux [W/m^2]	3000–180,000
Mass flux [kg/m^2 s]	209–1230

Table 2
Measurement uncertainty

Bulk fluid temperature [°C]	3.7%
Wall temperature [°C]	4.1%
Absolute pressure [MPa]	±0.01
Heat flux [W/m^2]	1.0%

measure conduction to the non-heated region of the test channel, two thermocouples were attached upstream of the starting position of the heating region. Fluid temperature was measured at the inlet and outlet of the test section using the same kind of thermocouples. The bulk fluid temperature at the outlet was measured in an outlet mixing chamber. The thermocouple wire was calibrated using an RTD (resistance temperature detector) with ±0.1 °C accuracy.

The outer wall temperatures were measured for various experimental conditions with inlet temperature, heat flux, and mass flux within the ranges shown in Table 1 at the constant system pressure of 8 MPa. The Reynolds numbers based on the inlet conditions, $Re = \rho_b u_b D_{hy}/\mu_b$, were in the range of 30,000–140,000, and the Grashof numbers, $Gr = g\beta_b q D_{hy}^3/k_b v_b^2$, varied from 10^9 to 10^{11} based on the circular tube diameter.

The fluid enthalpy at any position on the test section was calculated from the measured values of the inlet fluid temperature, mass flow rate, and heat flux by an energy balance. Then, the bulk fluid temperature was determined from the calculated fluid enthalpy according to the carbon-dioxide property tables. Thermophysical properties were evaluated from NIST chemistry web book and NIST refrigerant properties database 6.0.

The measurement uncertainties are listed in Table 2. The average deviation of the measured fluid temperature of carbon-dioxide from the calculated value at the channel exit is found to be 3.7%. Considering thermocouple conduction [3], the uncertainty of the measured wall temperature is estimated to be 4.1% on the average with a maximum value of 6%. Thermocouples used to measure the channel wall temperature are exposed to ambient whose temperature is lower than the wall temperature. Therefore, the recorded wall temperature is lower than the true value because of heat loss from the thermocouple to the ambient surroundings.

3. Results and discussion

Fig. 2 shows the wall temperature distributions at five different heat fluxes for the three test channels at a same mass flux of 419 kg/m^2 s. It should be noted that for the

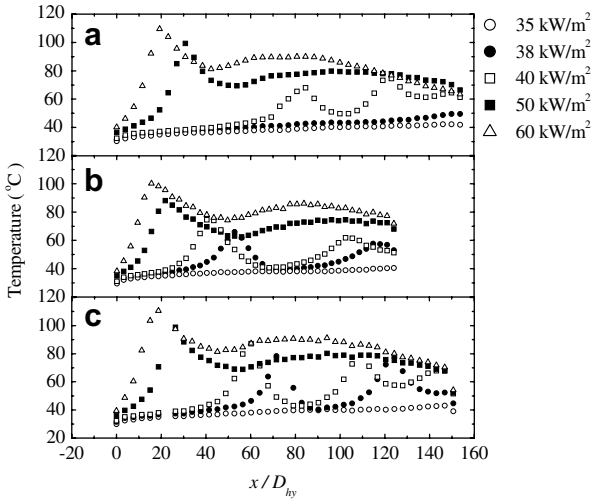

Fig. 2. Comparison of wall temperature distributions at a mass flux of 419 kg/m^2 s: (a) circular channel, (b) triangular channel, and (c) square channel.

non-circular channels, since the experiments were conducted at the same heat flux [kW/m^2] and mass flux [kg/m^2 s] as for the circular channel, the total heat input [kW] and mass flow rate [kg/s] are different because the flow passage and heating areas are different from one to another. The wall temperature variations for the non-circular channels along the streamwise direction show similar trends to those of the circular channel for the same heat flux and mass flux. The local peak in the temperature distribution indicates the occurrence of the heat transfer deterioration. For all channels, the heat transfer deterioration is clearly observed at heat fluxes higher than 38 kW/m^2. For the non-circular channels, the wall temperature peak appears earlier than for the circular channel at the lower heat flux. For example, when the heat flux is 40 kW/m^2,

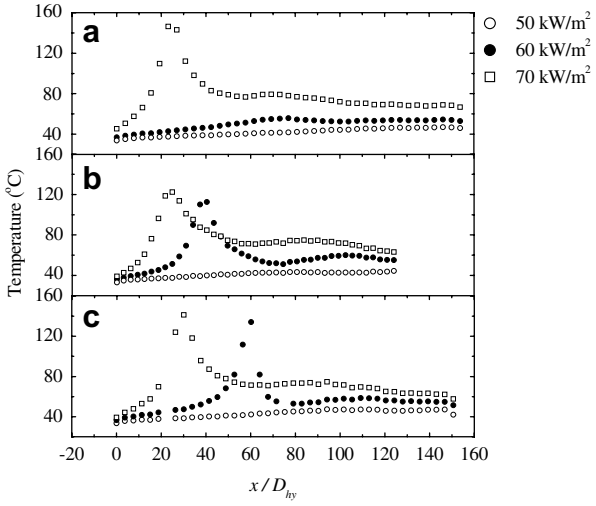

Fig. 3. Comparison of wall temperature distributions at a mass flux of 523 kg/m^2 s: (a) circular channel, (b) triangular channel, and (c) square channel.

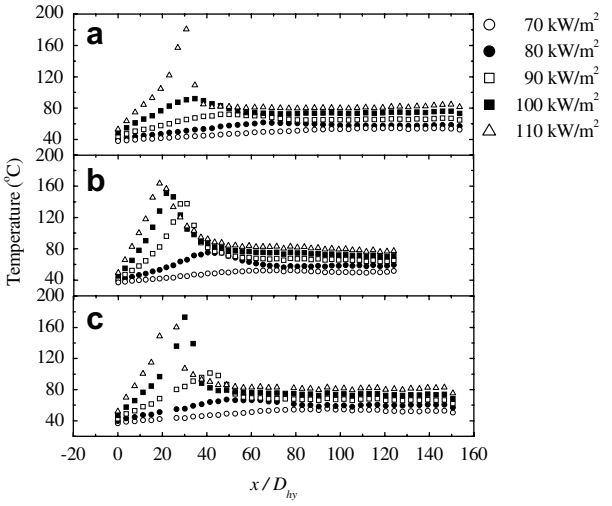

Fig. 4. Comparison of wall temperature distributions at a mass flux of 628 kg/m^2 s: (a) circular channel, (b) triangular channel, and (c) square channel.

the temperature peak appears at $x/D_{hy} = 40$, 60, and 85 for the triangular, square, and circular channels, respectively, whereas it occurs at about $x/D_{hy} = 20$ for all channels when the heat flux is 60 kW/m^2.

Fig. 3 compares wall temperature distributions at a mass flux of 523 kg/m^2 s. When the heat flux is 50 kW/m^2, no heat transfer deterioration is observed for all three channels. However, as the heat flux increases to 60 kW/m^2, the peaks in the wall temperature distribution can clearly be seen for the non-circular channels, while only a slow rise and fall in the wall temperature distribution appears for the circular channel. The heat transfer deterioration is a little delayed to the downstream region for the square channel at the heat flux of 60 kW/m^2, but it takes place about the same location as the heat flux increases to 70 kW/m^2.

When the mass flux is further increased to 628 kg/m^2 s as shown in Fig. 4, The temperature peak appears when the heat flux is larger than 70 kW/m^2, and a similar trend, as a whole, is apparent in the wall temperature variation with increase in the heat flux as in the case of lower mass flux. However, in the upstream region, the heat transfer deterioration is prominent in the non-circular channels at the heat fluxes of 90 and 100 kW/m^2.

4. Conclusion

Wall temperature variations for turbulent flow at supercritical pressure in circular, triangular, and square channels have been investigated experimentally. Data are presented for three different mass fluxes of 419, 523, and 628 kg/m^2 at various heat flux conditions. Regardless of the channel shape, the heat transfer deterioration occurs at the higher heat flux as the mass flux increases because of flow acceleration near the wall due to buoyancy, which suppresses flow turbulence. The distinctive characteristics in the wall temperature distribution of non-circular channels compared to those of circular channel are (1) The heat transfer deterioration is observed at a little lower heat flux at the same mass flow rate; and (2) in the regime of the heat transfer deterioration, the peak in the wall temperature distribution occurs earlier in the upstream region, but it takes place about at the same location as the circular channel at the sufficiently high heat flux.

Acknowledgement

The authors gratefully acknowledge that this work is supported by the Micro Thermal System Research Center, Seoul National University, through the I-NERI project.

References

[1] D.A. Campbell, H.C. Perkins, Variable property turbulent heat and momentum transfer for air in a vertical rounded corner triangular duct, Int. J. Heat Mass Transfer 11 (1968) 1003–1012.
[2] E. Battista, H.C. Perkins, Turbulent heat and momentum transfer in a square duct with moderate property variations, Int. J. Heat Mass Transfer 13 (1970) 1063–1065.
[3] J.P. Holman, Experimental Methods for Engineers, seventh ed., McGraw-Hill, 2001 (Chapter 3).